A new laboratory method to measure heat exchange in tensile fractures

Richard R. Bakker[1], David F. Bruhn[1,2] and Auke Barnhoorn[1]

[1] TU Delft, Civil Engineering and Geosciences, Stevinweg 1, 2628 CN, Delft, the Netherlands

[2] GeoForschungsZentrum (GFZ) Potsdam, Telegrafenberg, Building A 69,

14473 Potsdam, Germany

r.r.bakker@tudelft.nl

Keywords: Mode 1 Fracturing, Heat exchange, experimental, rock deformation.

ABSTRACT

Recently the focus of geothermal engineering has shifted towards "ultra-deep" geothermal systems (considered as more than 4 km depth in the Netherlands). At such depths there is a high lithostatic load, which may in turn have caused significant compaction to potentially porous reservoir rocks. As an alternative, open fractures (with sufficient aperture) could form an alternative fluid pathway. Such fractures can arise as a result of a tectonic phase, and subsequent relaxation, as well as during a tectonic phase.

Existing 'hot' fluids in such pathways are brought up to the surface, thermal energy is extracted and subsequently the fluids are pumped back into the subsurface. The cold fluid can potentially be reheated, and cycle through the system, for as long as there is enough thermal energy absorbed by the fluid. The operational lifetime of such a system depends on a number of variables, including the surface area of heat exchange, overall flow-rate and local fluid velocity.

To investigate the effect of faults surface roughness, which affects surface area, on the permeability and heat exchange capacity of such fractures, we designed laboratory experiments performed at elevated pressures and temperatures. For this purpose, we have adapted a conventional tri-axial apparatus. Pistons are modified to apply a line-load to a cylindrical sample forcing the sample to split along its long axis. These pistons can also be used to keep the fracture "wedged" open at a given aperture. When a sample is split, we cycle water through the fracture and heat the assembly up. Subsequently we flow cold water through the sample at a known flow-rate, and measure the temperature evolution at thermocouples within the pore-fluid lines close to the sample. Additionally, after the test we are able to determine surface area and fracture roughness by means of micro-CT analyses.

Initial results indicate that while variation in fracture surface area may influence permeability, it leads to only minor changes in heat exchange. We find that the combination of conductive heat flow within the rock mass and the flow rate of the fluid controls temperature evolution over time in geothermal fractured systems.

1. INTRODUCTION

Geothermal energy is likely to play a major role in the "energy transition", where fossil energy sources (high-carbon) are replaced by low-carbon emission solutions. Current systems already in use in the Netherlands (e.g., Bonté et al., 2012) are mostly well doublets in hot sedimentary reservoirs (e.g., van Wees et al., 2012). Such porous systems are somewhat limited to shallow depths as at high lithostatic stress, pore space can be reduced due to compaction effects (e.g., Vajdova et al., 2004; Baud et al., 2012; Brantut et al., 2013). Deeper systems have a higher energy potential (due to the geothermal gradient), but suitable fluid pathways (i.e., permeable structures between injector and producer) are difficult to find. In the context of the Dutch subsurface, the focus lies on fractured media, primarily on fossil, inactive fault systems (e.g., Loveless 2014). These may not have sufficient permeability and should be somehow stimulated in order to be viable targets for geothermal exploitation. Engineering of such a Geothermal System (EGS) requires knowledge on the physical properties of rocks, such that detailed models of sub-surface mechanics can be built (e.g., how are current fracture apertures affected, are new fractures generated). Additionally, to assess the amount of energy that can potentially be extracted, robust estimates on heat exchange between rock mass and (working-)fluid are needed. Such models require input from laboratory tests that are ran at representative confining pressure and temperature. Moreover, in laboratory tests, certain parameters (such as fracture aperture) can be systematically varied and repeated, which is difficult in field settings. Furthermore, samples can be recovered analysed in detail after testing.

Here we present a new type of laboratory test, designed to assess the creation of opening tensile

fractures within a conventional triaxial deformation apparatus. This method has the benefit over standard tensile test procedures (such as the Brazilian disk indirect tensile strength method (e.g., Guo et al., 1993; Paterson and Wong, 2005) and direct tensile strength tests (e.g., Perras and Diederichs, 2014) that it can be run in a confined setting, i.e., with compressive stresses as boundary conditions. Using the novel setup, the newly created fracture's aperture can be systematically varied, and its effects on heat exchange studied by means of thermocouples fitted within the pore fluid system. Moreover, this setup uses intact starting material, thus avoids the need to fracture the rock prior to testing in a different apparatus, and thereby risk of loss of material and/or the risk of displacing the two sample halves relative to each other causing additional fractures. We present here some initial findings as the method is developed and compared with numerical models, and discuss the applicability to accurately measure heat-exchange in tensile fractures.

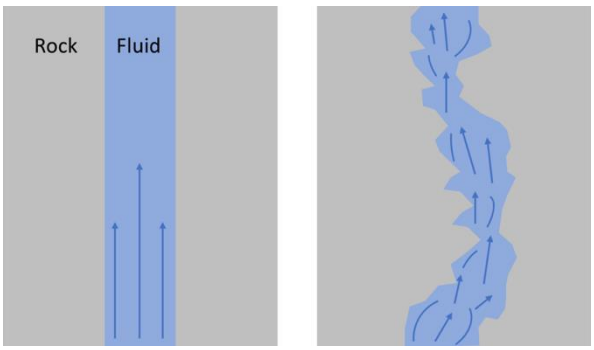

Figure 1: Illustrating the main hypothesis of this work: natural fractures (depicted left) have more turbulent flux, which affects heat exchange compared to regular (straight) fractures (depicted left).

2. EXPERIMENTAL SETUP

2.1 Apparatus

We used a triaxial deformation apparatus as installed in the Geoscience and Engineering department of Delft University of Technology. This machine is commonly used for tests on right-cylinders, and is capable of deforming samples of various sizes at a confining (radial) pressure of up to 70 MPa, with maximum axial load up to 300 kN. Maximum axial stress depends on sample diameter, for a 30 mm diameter core this would result in a maximum stress of

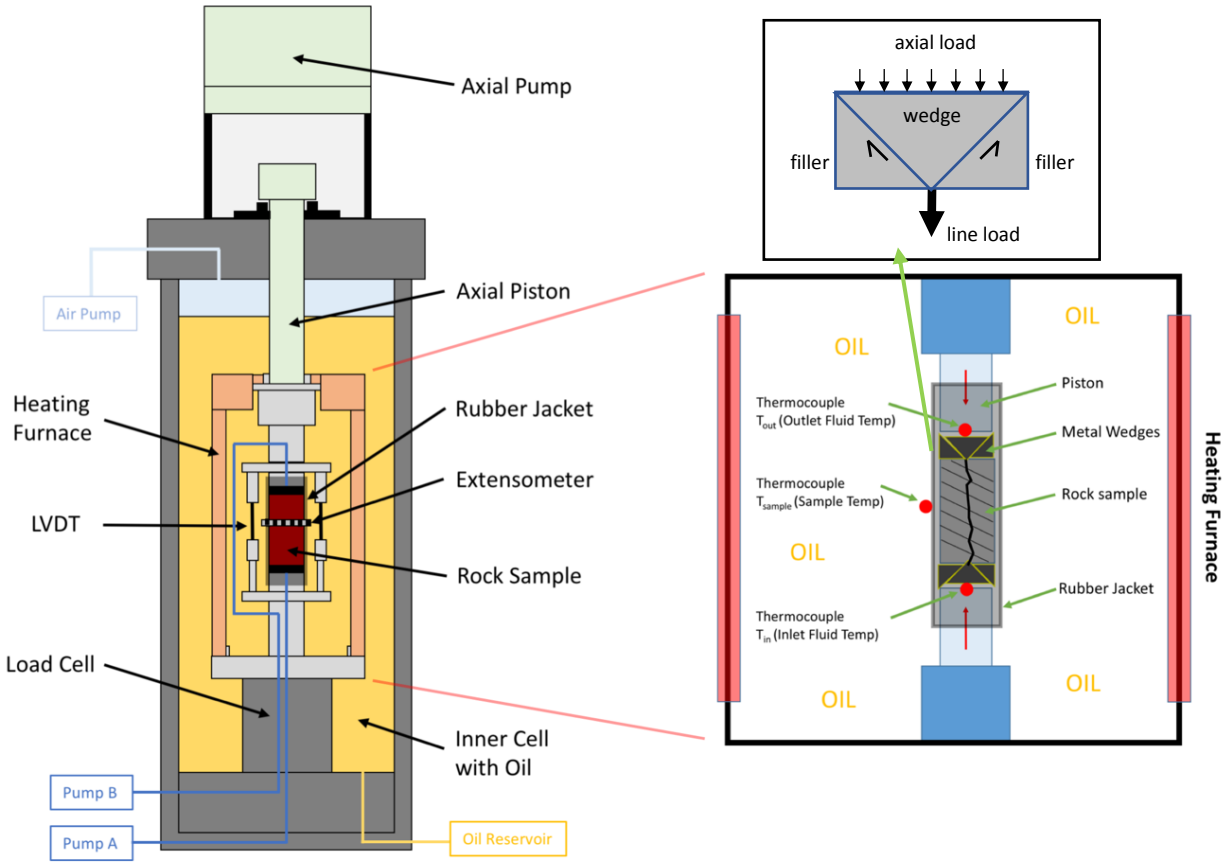

Figure 2: Schematic of the triaxial cell (left), the sample assembly (right) with detail of a wedge setup (inset, above)

424 MPa. Axial strain is calculated from two Linear Variable Differential Transducers (LVDT), placed parallel to the sample setup. Radial strain is calculated from chain-gap LVDT data, where the chain is span around the axial middle of the sample. The sample is squeezed between axially mounted steel pistons, which are fitted with pore fluid lines, and gridded to allow equal distribution of fluids through the sample edges.

Instead of a normal right-cylinder with a standard length to diameter ratio (commonly 2.5:1), we use shorter samples (ratio 5:3) and use the extra space to fit wedges and fillers (see inset figure 2) made out of hardened steel (see figure 2). The fillers can slide along the sample and the wedges, and allow for a hydrostatic state of stress on the sample due to the radial stress. Between the wedges and the fillers, a thin layer of non-solvable grease is applied to reduce friction effects. When there is an increased axial load, the wedges push down, thereby displacing the fillers outward and essentially producing a line load on the top and bottom faces of the sample. This can be used both to create a mode 1 fracture (similar to the line load in Brazilian disk testing) as well as to keep a fracture open at a certain aperture, by the interplay of radial stress and axial load. Inside the wedges there are small holes to allow fluid flow to and from the sample (fracture).

The sample is isolated from the confining medium (high temperature resistant oil) using a 2 mm thick EPDM-rubber jacket. This thickness ensures that the seal remains intact during fracturing of the rock (i.e., the jacket does not tear on fracture edges due to being squeezed into the newly created void). However, it does introduce an error on the fracture aperture as the jacket is stretched, and thereby the jacket wall thins. We correct for this effect by assuming a constant cross sectional area.

The sample and pistons are placed within a furnace, that is able to heat up the assembly to a maximum of 200 ˚C, as measured through a thermocouple placed inside the furnace. To get more accurate temperature readings, a second thermocouple is placed directly on the middle of the sample, outside of the jacket. In addition, thermocouples are placed inside the pore fluid access lines in the steel pistons, such that the temperature of the fluid entering and exiting the sample space can be measured.

The pore fluid lines are connected via high-pressure lines to a set of external high precision syringe pump units (Teledyne Isco 100DM).

2.2 Samples

We used “Odenwald Granite”-samples, representing basement rocks as found in upper crustal conditions (most commonly below the sedimentary cover). All samples were cored from a single block of in-tact material (i.e., no fractures were observed with the naked eye). The block originated from a quarry in Odenwald, Germany (RÖHRIG Granit GmbH, GPS coordinates (N;E): 49.633071; 8.700709). The material is coarse-grained crystalline (quartz, biotite and plagioclase crystals) and visible minerals up to 5 mm in equivalent diameter size. Comparable intact granitic rocks were found to have a porosity of about 0.8% (helium pycnometry) and permeability less than the detection limit of the triaxial apparatus: less than 10^{-18} m^2. Thermal properties (conductivity and effusivity) were determined using a C-Therm Thermal Conductivity Analyzer® as installed at the Material Physics Laboratory, at the Aerospace Engineering Faculty of TU Delft. This analyzer consists of a metal spiral on a flat surface where a sample half-space (effectively a flat surface and a height of at least 5 mm) is placed. Wetting (with distilled water) of the contact surface ensures no void space (air) between the measuring surface and the sample. A metal spiral is heated by a few degrees Celsius, and the subsequent thermal response of the sample is measured by adjacent temperature sensors. In this way the thermal effusivity as well as the conductivity are directly measured. The resulting parameters are averaged over 10 heating-cooling cycles. Heat capacity is derived from the density, effusivity and conductivity measurements. The thermal properties of the intact material are listed in table 1.

Table 1: Material properties measured on intact material

Property	Value	Unit
Density	2746	kg/m^3
Thermal Effusivity	2444	$W*s^{1/2}/m^2/K$
Thermal Conductivity	2.918	W/m/K
Heat Capacity	745.7	J/kg/K

2.3 Test procedure

After placing the samples in the apparatus, samples are subjected to a stepwise increasing radial stress up to 10 bar. The axial load is manually adjusted (increased) such that the distance between the wedges (as measured by the axial LVDT’s) remain constant. In practise this meant the axial load is comparable to the load that would be required in a standard triaxial test (i.e., 7 kN for a axial stress of 10 MPa on a 30 mm diameter sample). To ensure samples could be fractured at moderate loads, the confining pressure was kept relatively low. Thereby the chance the jacket remained intact during fracturing was high.

After this initial loading phase the samples were axially loaded to force the mode 1 fracture, and subsequently keeping the fracture open by keeping the wedges in place. As the friction contact between the wedges and samples are not well constrained, the axial load data can only be used as indicative values, and further testing is required to analyse the mechanical data.

From the initial loading phase onward the sample is vacuumed, followed by flushing with CO_2 at low pressure, from is set on the upstream side of the pore fluid system. As the sample is considered impermeable on the experiment timescale (~8 hours) no notable amount of gas migrates through the sample. However, when gas is able to migrate to the downstream side through the sample, and a clear jump in the radial strain data is observed, we consider the sample fractured.

After flushing with CO_2 the sample is flooded with distilled water. Additional CO_2 still residing in the sample is dissolved by pressurising the pore fluid to 1 MPa. The sample is flushed with at least one full stroke of the syringe pumps (100 mL), after which the water is replaced with fresh distilled water, free of CO_2.

When the sample is fractured and filled with fluids, the whole assembly is heated up to ~100 ˚C. Due to the design of the furnace, achieved temperatures in the upper piston line closely match the furnace temperature, but the temperature in the lower piston is significantly less. However, to simulate a geothermal system (where hot water is pushed out by cooled down reinjected water), this does not pose a problem as cold water with a known temperature is introduced into the sample, and the heat-exchange can still be quantified. Moreover, upper piston has a pore fluid line that runs along the sample assembly through the furnace, and would be heated up while flowing. Flowing from the lower to upper piston therefore yields a higher temperature difference. On the downstream side (upper piston) one of the two fluid pumps is set to constant pressure mode (i.e., constant back pressure). On the upstream side (lower piston) the second pump runs at a constant flowrate. This flowrate is step-wise varied in order to assess how effectively the water is cooling down the sample.

2.4 micro-CT imaging

To assess the fracture geometry samples were imaged in 3D using a Phoenix NANOTOM high resolution micro CT (computed tomography) scanner, located in the Geoscience Laboratory at TU Delft. The scanner uses an x-ray-source with a maximum voltage of 180 kV and maximum power of 15 W. The minimum focal spot size is ~ 0.9 µm, maximum sample diameter is 120 mm and maximum mass approx. 1 kg. The resolution depends on the sample size and can be as low as 1 µm for a sample size diameter of 1 mm. Due to that the sample is thicker in the middle than the edges, a correction for beam hardening (factor 9) is applied.

Image slices from the tomography are subsequently analyzed in commercially available image analysis software “Avizo” (ThermoFisher Scientific). Fracture geometry is extracted by cropping the images, such that only the sample is analyzed, and subsequent segmentation based on interactive thresholding. From the fracture-geometry we extract the gap-volume (unconfined) and surface area. These are used in combination with the triaxial tests to assess their effects on heat exchange.

3. RESULTS & DISCUSSION

For all experiments a significant temperature gradient across the sample was found once the furnace had stabilised at a constant temperature. When the centre of the sample and the upper piston were around 100 ˚C (similar to the furnace temperature), the lower piston was found to be at 60 ˚C. While this prevents a quantitative estimation of the heat exchange, systematic changes by varying flow rate and aperture of the fracture could be deducted. A typical experiment run is shown in figure 3, and detail in figure 4.

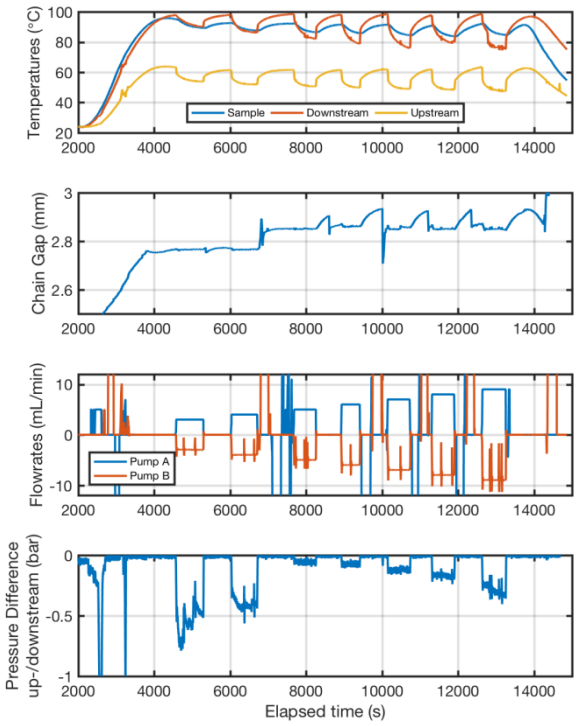

Figure 3: Example of a typical experiment run, (experiment 4) where the sample was cooled down by flushing water through the sample at different flowrates, with ample time for the sample to heat back up between runs. All panels share the same x-axis (elapsed time in seconds). From top to bottom: Temperatures (in degrees Celsius) at three main locations (upstream, downstream pore fluid lines and outside of the sample); Chain gap LVDT (in millimetre), as proxy for the fracture aperture that was manually kept constant by adjusting the axial load; Flowrate of both pumps in millilitre per minute (including spikes caused by refilling and removing water); the measured pressure difference between up and downstream in bar (negative values indicate higher pressure on upstream side).

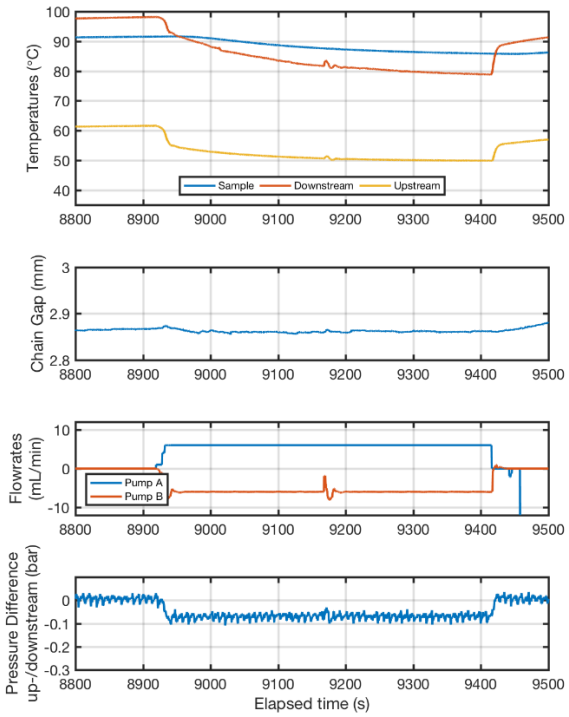

Figure 4: detail of figure 3, with similar panels, showing data at a flowrate of 6 mL/min and the exponential decay of temperature can be observed. Notice how the chain gap is kept within 0.05 mm, thereby implying the fracture aperture does not vary more than that. The spike in pump B (red line, 3rd panel from the top) is due to an instability (and reset) of the PID controller inside the pump unit (maintaining constant pressure).

For a period with constant flow rate, we observe an immediate drop of temperature at the upstream, whereas a similar drop is somewhat delayed on the downstream side. This is most likely due to the volume of hot water inside the fracture that is still hot, and displaced first. After this the temperatures decrease over time towards a certain equilibrium. We chose to stop the flow after approximately 10 minutes, both as the pump volume is finite, and to avoid a significant response (in terms of heat flux) of the furnace. The furnace is programmed to be relatively slow in responding to temperature changes by tuning the PID settings the furnace controller, such that the temperature of the furnace can be considered a constant heat flux for a period of 10 minutes, as well as constant temperature boundary condition.

As temperatures change during flow, the wedges themselves would also cool down. This in turn caused thermal contraction which led to an observed decrease in fracture aperture. This effect was counteracted by manually increasing the axial load. After flowing water through the fracture, the sample would heat back to the prior equilibrium state, and the axial load was decreased to allow the fracture aperture to remain constant. However, due to manual control this was prone to over- and undershoot effects.

3.1 Effect of flowrate

We observed higher temperature changes (defined as the temperature before flowing, compared to 10 minutes of steady state flow) with increasing flow rates. All of these experiments were done at comparable fracture permeability, as evidenced by the resulting pressure differences. With the assumption of comparable fractures, we group the data from these experiments together and observed a linear relation between flow rate and absolute temperature change. However, extrapolation to a flow rate of zero should theoretically lead to a temperature change of zero. This is the case for the outflow, but does not seem to be the case for the inflow. On the other extreme, a very high flow rate, the temperature can only change from 100 ˚C to the temperature of the water in the pump (ambient, 20 ˚C) and heating effects due to flow in the pore fluid lines and sample are negligible as the "retention"-time of the fluid is almost zero. In this case the upper limit of the temperature change should asymptotically be bounded by approximately 80 ˚C. The linear trendline depicted in figure 5 should perhaps be seen as a linear section of a more complex function as the linear line doesn't have asymptotes. Moreover, the results depicted here are valid for our specific sample size and time scale, with fracture width and length of approximately 30mm and 50 mm respectively.

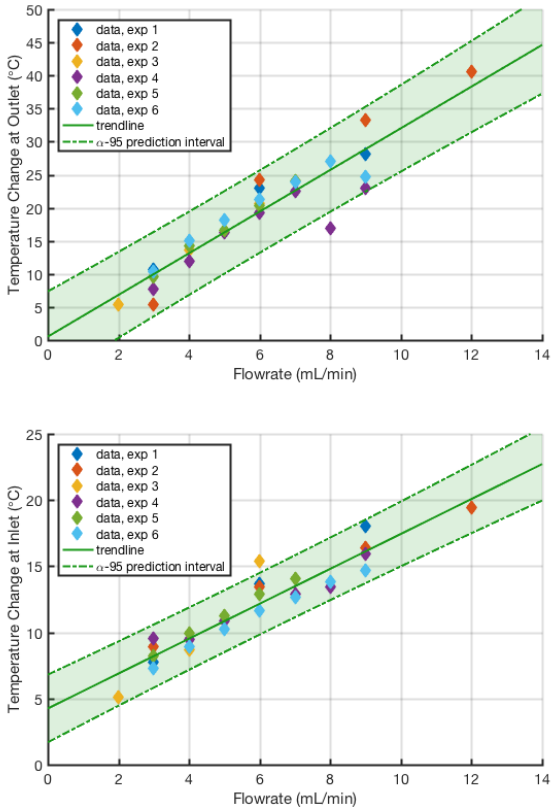

Figure 5: Absolute temperature change after 10 minutes at inlet (upstream) and outlet (downstream) for different flow rates. The data has been grouped together and fitted with a linear function. The prediction interval zone (based on a 95% confidence interval) is depicted by the green zone.

3.2 Effect of aperture

Varying fracture aperture did not result in notable changes in observed temperature changes, at least not for the range that could be achieved here (see figure 6). A slight downward trend can be observed, but that falls within a wide prediction (alpha = 95%) interval, indicating the linear fit is uncertain. A larger fracture aperture would mean that more hot fluid initially resides in the fracture, and thereby the period before the temperature at the outflow starts to drop would be longer. However, we speculate there is a trade-off, as the flow velocity next to the fracture is lower, thereby allowing more time for the water to heat up.

Conversely, with lower fracture apertures (that were avoided in the experiments here due to low permeability and thereby high effective stress gradients across the sample), the fluid velocity would be higher, allowing less time for the water to heat up. Based on our results we cannot distinguish notable effects of fracture aperture.

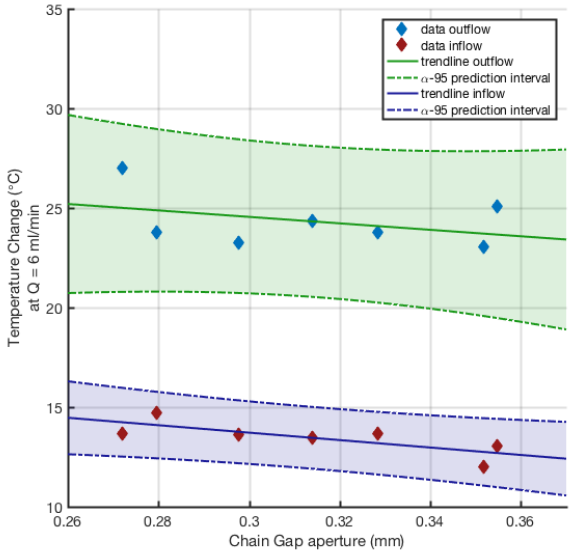

Figure 6: Absolute temperature change after 10 minutes at inlet (upstream) and outlet (downstream) for different fracture aperture, as measured by the chain gap LVDT. The data is derived from a single experiment to avoid variation caused by fracture geometry. The prediction interval zone (based on a 95% confidence interval) are depicted by the green and blue zones.

3.3 Geometry

All experiments yielded a near-straight fracture from top to bottom of the sample. An example is shown in figure 7. In most cases a single fracture was formed, with the exception of experiment 6. Derived fracture parameters are listed in table 2. Similar to the effect of aperture, notable differences in cooling behaviour between experiments was not found, even not for experiment 6 with a larger surface area.

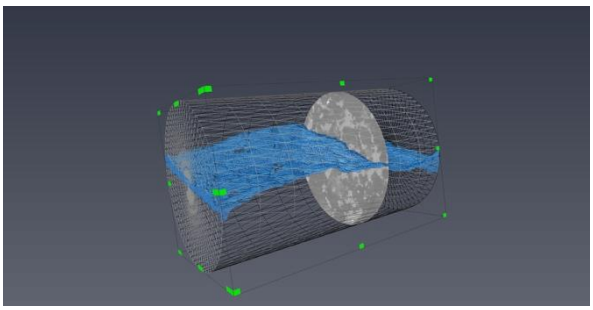

Figure 7: Example of the post-processing in Avizo software. Depicted are a single raw image slice (grayscale) and the final fracture geometry (in blue). The cylindrical grid represents the volume in that was used for interactive thresholding. Voxels outside this volume was ignored. Sample size is indicated by the bounding cylinder grid: a cylinder of 30mm diameter and 50 mm length.

Table 2, Fracture gap volume and surface area as derived from microCT imaging and subsequent image analysis in Avizo. Note that the volume is when the rock is unconfined and the aperture is therefore much higher. Values posted here to allow comparison between different fractures. Experiment 6 has notably higher values for volume and surface area, which is due to the fact that in this experiment two fractures were formed.

Experiment	Volume [mm^3]	Surface [mm^2]
1	765.1	4790.2
2	769.7	5516.3
3	743.8	3692.2
4	1082.7	4556.7
5	1074.2	5036.8
6*	1528.5	9722.2

3.4 General law for cooling?

The question arises whether surface area is an important parameter. The advection of heat by means of flowing water in the fracture could be the most efficient step in the heat-transport chain. Another component in that chain is the heat conduction in the rock. In other words, if heat can't be supplied fast enough, the water will just flow by without heating up significantly. This could explain the observed positive relation between flow rate and temperature change: the water simply flows too fast to pick up more heat. Moreover, in all cases we observe an exponential cooling that could be well compared by Newton's law of cooling. This law states that the rate of change of the temperature of an object is proportional to the difference between its own temperature and the ambient temperature (i.e. the temperature of its surroundings). This generally works well for cooling that is limited by conduction. Considering the temperature of the inflowing water stays relatively

constant after about 1 minute, a constant surrounding temperature at the fracture interface can be assumed. The temperature drop at the outflow side implies that less heat is extracted, which corresponds well to Newton's law of cooling. Assuming all heat is derived from the rock sample, this indicates the process is limited by the heat conduction of the rock.

As noted before, due to the temperature gradient in the apparatus we've used in this study, no quantitative description of the cooling (and thereby heat extraction and heat exchange) is made. However, qualitatively we can show that temperature decay is remarkably similar to Newton's law of cooling. This law takes the general form:

$$T(t) = T_e + (T_0 - T_e) \times e^{-kt} \quad [1]$$

Where T(t) is the temperature over time, T_e is the ambient (environmental) temperature, T0 the initial temperature and –k a constant governing the rate of cooling

Using the general form from equation 1, we fit the data as shown in figure 8. We find the environmental (final) temperature is 78.80 ˚C for this particular flowrate (6 ml/min), and a temperature difference (T_0-T_e) of 17.81 ˚C. This would imply the sample started cooling at 96.61 ˚C while in fact a slightly higher temperature is measured. However, if the temperature of the inflowing water may be taken as a measure of T_e, it is clear that this value is not constant. Thus while fitting the data with a Newtonian law of cooling works well from a mathematical point of view, the physical process is more complex given the large thermal gradient due to the furnace used in the triaxial vessel used for this work. That said, the measurement principle is demonstrated, and qualitatively it is clearly indicated that heat conduction plays an crucial role in the cooling of the rock sample.

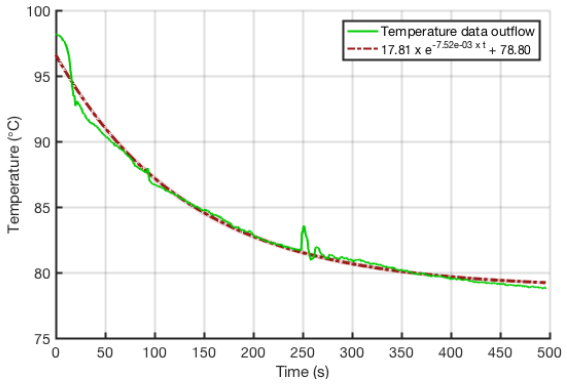

Figure 8: Example of fitting the outflow temperature data using an exponential decay function of type a x exp(b x t)+c. Raw data is taken in from the time window depicted in figure 4, and shown here as the green line. The exponential fit is shown in as red dashed line. The prediction interval zone (based on a 95% confidence interval) is depicted by the red zone, but is quite narrow due to the good fit.

4 CONCLUSION

As naturally produced fractures have a higher surface area compared to straight planar models of fractures, the heat exchange process could potentially be different. We have developed a new method to study the process of heat exchange inside a tensile, opening fracture at reservoir pressure and temperature condition using a conventional triaxial deformation apparatus. We use a novel setup with specially designed wedges that are used to impose a line-load across the sample length causing the rock to fracture much like with the conventional brazil-disk method. Moreover, the wedges can be used to maintain a fracture aperture. Thermocouples are fitted inside the pore fluid system such that the temperature of water entering and exiting the sample space can be monitored through time.

After fracturing the newly formed fracture is filled with water and heated up, followed by multiple stages of flow through the sample, varying flowrates and aperture. At each stage water temperature at the inflow of the sample would immediately drop, followed by a more gradual cooling over time as the water that flows through the apparatus is still heated up slightly. At the outflow point, the temperature drop is somewhat delayed, as water inside the fracture is flushed out first. This is followed by a decrease in temperature that is best described by an exponential decay function. Comparing outflow temperature after a period of constant flowrate (10 minutes), we observe a linear relation, with higher flowrates corresponding to lower temperatures. With higher flowrates the temperature difference between the water and the rock face is larger, thereby more heat is conducted out of the sample. We did not find significant effects with fracture aperture, but note that the aperture in our experiments is quite wide, to avoid large effective stress gradients in the sample due to low permeability.

Our initial findings show that the amount of heat that can be extracted by fluid flow along fractures is limited to the thermal conductivity of the solid medium (rock). Because heat conduction is the slowest factor in the heat transport, flow rates in fractures (at sufficient aperture) do not play a significant role. The amount of heat that can be extracted from the rock mass can be well approximated by a general Newtonian-cooling type law. However, further experimentation is required to further constrain this in terms of quantitative values. This could possibly be achieved by a dedicated tri-axial vessel with an improved furnace design, such that temperature gradients across the sample length are avoided.

REFERENCES

Baud, P., Meredith, P., & Townend, E. (2012). Permeability evolution during triaxial compaction of an anisotropic porous sandstone. Journal of Geophysical Research: Solid Earth, 117(B5).

Bonté, D., Van Wees, J. D., & Verweij, J. M. (2012). Subsurface temperature of the onshore

Netherlands: new temperature dataset and modelling. Netherlands Journal of Geosciences, 91(4), 491-515.

Brantut, N., Heap, M. J., Meredith, P. G., & Baud, P. (2013). Time-dependent cracking and brittle creep in crustal rocks: A review. Journal of Structural Geology, 52, 17-43.

Guo, H., Aziz, N. I., & Schmidt, L. C. (1993). Rock fracture-toughness determination by the Brazilian test. Engineering Geology, 33(3), 177-188.

Loveless, S., Pluymaekers, M., Lagrou, D., De Boever, E., Doornenbal, H., & Laenen, B. (2014). Mapping the geothermal potential of fault zones in the Belgium-Netherlands border region. Energy Procedia, 59, 351-358.

Paterson, M. S., & Wong, T. F. (2005). Experimental rock deformation-the brittle field. Springer Science & Business Media.

Perras, M. A., & Diederichs, M. S. (2014). A review of the tensile strength of rock: concepts and testing. Geotechnical and geological engineering, 32(2), 525-546.

Vajdova, V., Baud, P., & Wong, T. F. (2004). Permeability evolution during localized deformation in Bentheim sandstone. Journal of Geophysical Research: Solid Earth, 109(B10).

Van Wees, J. D., Kronimus, A., Van Putten, M., Pluymaekers, M. P. D., Mijnlieff, H., Van Hooff, P., ... & Kramers, L. (2012). Geothermal aquifer performance assessment for direct heat production–Methodology and application to Rotliegend aquifers. Netherlands Journal of Geosciences, 91(4), 651-665.

ACKNOWLEDGEMENTS

This work is carried out in partial fulfilment of the MSc. degree of Marco Balmer. The work is funded within the EU Horizon 2020 research and innovation programme under grant agreement No. 654662 (named “SURE”). The authors would like to thank the technical staff of the TU Delft Rock Mechanics laboratory, particularly Marc Friebel (initial design and manufacturing of anvils) and Ellen Meijvogel - de Koning (micro CT scans).